Numerical Flying-Height Modulation Due to Disk Clamping Distortions and Flutter

Brian H. Thornton and D.B. Bogy
Computer Mechanics Laboratory
Department of Mechanical Engineering
University of California
Berkeley, CA. 94720

Abstract*—When modeling the affects of the disk clamping distortions, flutter and warpage on flying-height modulation (FHM), we found that significant numerical error was introduced. In fact, this numerical error was found in some cases to be as large as 36 % of the flying height (FH). This error in numerical FHM originated from the time-step digitization of the disk's surface underneath the slider from a continuous sinusoid to a series of sloped step functions. An equation is derived that predicts this numerical FHM from the step heights between the adjacent time steps of the disk's profile. This "numerical FHM" is proportional to the time step, the relative linear velocity between the slider and the disk's surface, and the amplitude of the waviness, and it is inversely proportional to the waviness wavelength. The derived equation was tested with various simulations, and it shows high prediction accuracy for disk waviness wavelengths much longer than the slider's length. Therefore these erroneous FHM results occur when modeling long wavelength disk clamping distortions and flutter. To overcome this erroneous result we should either not model the disk clamping distortions and flutter when investigating FHM, minimize this affect by decreasing the time step or remove this numerical FHM by use of the derived equation post-simulation. It was also found that a time step of 0.0001 ms or less is needed to accurately capture geometric FHM that results from the disk morphology.

I. INTRODUCTION

As the FH decreases to keep up with the demand for the rapid increase in magnetic areal densities, a better understanding of the head-disk interface (HDI) is needed. With the physical spacing between a read-write element and the magnetic disk surface approaching 5 nm or less, any fluctuations in the FH could cause catastrophic failure. The Computer Mechanics Laboratory (CML) Dynamic Air Bearing Simulator can be used to numerically simulate the HDI with high accuracy when used properly. However, as with any numerical simulation it is necessary to understand the errors when discretizing a continuous system. Furthermore, the numerical errors need to be minimized for the specific simulation and the particular results of interest.

FHMs resulting from disk clamping distortions, flutter and warpage raise concern due to the inherent spectral content of these disk non-planar displacements as the disk spins under the stationary slider. In general, for all disk substrates, whether glass, aluminum or some ceramic material, the spectral content of the disk's clamping distortions, flutter, warping, waviness, micro-waviness, and roughness show an exponential decay with decreasing wavelength. With current pico sliders flying at sub-20 nm with high air bearing stiffness and suspensions with relatively low stiffness, the theory of linear dynamical systems would not be expected to produce significant FHM during "steady" flying conditions in the frequency bandwidth of DC up to the first air-bearing resonance. However, we have found that for wavelengths below about 2-3 times the slider's length, FHM starts to become pronounced due to geometric effects [1]. In this paper we are concerned with wavelengths in this range and larger. Numerical solutions obtained using the CML Dynamic Air Bearing Simulator can predict that FHM

exists due to disk clamping distortions, flutter, and warping with significant amplitude – up to 36 % of the FH. However, these erroneous results are found to be due to numerical error – they are not physical. This error is caused by the discretization of the disk's surface from continuous sinusoids to digitized step functions. To explain this phenomenon a simple equation is derived, which can also predict this erroneous FHM. This numerical FHM is proportional to the amplitude of the out-of-plane disk motion, the relative linear velocity between the slider and the disk's surface, and the time step, and it is inversely proportional to the wavelength of the out-of-plane disk motion.

The numerical simulations show a linear relationship between the FHM and the relative linear velocity, waviness amplitude, wavelength and time step. Two-times and ten-times around disk clamping distortions and flutter were simulated to show the relative linear velocity and time step dependence, respectively. These simulations also show that as the time step approaches zero, so does the FHM. Also, a realistic amplitude disk function was generated that sweeps through frequencies corresponding to once around up to 50-times around disk clamping distortions and flutter. It was found for time steps of 0.0003 ms and larger the simple derived equation accurately predicts the numerical FHM due to disk waviness wavelengths down to 6 mm. For a time step of 0.0001 ms the derived equation accurately predicts the numerical FHM due to disk waviness wavelengths down to 16 mm. Below disk waviness wavelength of 16 mm the presence of geometric FHM starts to become pronounced and was modeled accurately by numerical simulations below a wavelength of 6 mm with a time step of 0.0001 ms or less.

Experiments were conducted to obtain supporting evidence for the explanation of the findings from the simulations. However the experimental system used, which has

very high repeatability above 10 kHz, is not accurate enough for measurements at frequencies below 7 kHz. In this frequency range an error of ± 5 nm is introduced, therefore making it impossible to accurately measure FHM due to disk clamping distortions.

II. DISK DYNAMICS

The first spectral component of the out-of-plane (normal to the disk's surface) displacement of a spinning disk, as seen by a stationary slider, is the fundamental rotational frequency, ω_o, due to non-perpendicularity of the disk to the spindle. The next frequency component is twice the fundamental rotational frequency, $2\omega_o$, commonly called the "potato chip" clamping distortion of the disk as can be visualized in Fig. 1. Several discrete frequencies resulting from wind excitation, spindle ball bearing imperfections and other external excitation forces can excite many natural vibration modes of the disk [2]. Two additional disk mode shapes and frequencies are shown in Figs. 2 and 3 for a 95 mm diameter aluminum disk. The (*n*,*m*) labeling convention for the disk mode shapes designates *n*-nodal circles and *m*-nodal diameters [2]. Generally, the out-of-plane disk displacement amplitude due to the disk vibration modes decreases rapidly for higher disk vibration modes (as *n* and *m* increase). Another component of the spinning disk's out-of-plane displacement seen by the slider is the disk's surface morphology, including waviness, micro-waviness, and roughness. The disk's morphology generally displays exponentially decaying amplitudes with decreasing wavelength [4].

We are primarily concerned here with the low frequency content of normal disk displacement from DC to 10 kHz as depicted in Fig. 4. This figure contains the frequency domain averaged spectral content of the out-of-plane vibration of a typical disk from 0 to 10 kHz spinning at 10,000 RPM measured with a laser Doppler vibrometer (LDV). In this frequency band, the major spectral components are due to disk clamping distortions, spindle motor vibrations, and disk flutter due to windage excitation of the forward and backward traveling disk modes [2]. Figure 5 depicts these same LDV measurements of the out-of-plane motion of the disk as a function of RPM plotted as a "waterfall" plot. Here it is seen how the different disk mode shapes split into forward and backward traveling waves as RPM is increased with a slope approximately equal to $\pm n$ [2,6,7]. Also, spindle motor vibrations, clamping distortions, and ball bearing defect excited modes emanate from the origin and increase linearly with increasing RPM [2,7].

III. SIMULATING THE DISK SURFACE

When conducting dynamic simulations with the CML Dynamic Air Bearing Simulator, there are several different methods for incorporating the disk's motion. One method is to include the disk's motion by enabling in the simulator the 'disk generation of topography' with 'disk waviness/texture.' Another and very similar method is to enable the 'disk flutter' option in the simulator. Both methods generate similar disk topographies with a defined amplitude and wavelength or frequency similar to that seen in Figs 1 and 2. Arbitrary topographies can also be incorporated into the simulator with the 'point-by-point disk track profile.' Actual disk topography can be measured with a LDV or other measurement methods to obtain the actual disk motion as it spins under the

slider. There are other options in the simulator that can be used to simulate other types of disk or slider motions/morphologies, however, here we will only discuss those mentioned above.

The first two methods can be used to incorporate the disk clamping distortions and disk flutter, and the third method can be used for the disk morphology. Therefore all of the out-of-plane motion of a disk can be incorporated into the CML Dynamic Air Bearing Simulator, and dynamic simulations can be carried out to determine how the actual motion of the disk affects FHM.

In the numerical simulation, a continuous system is discretized into discrete space and time steps. In order for the results to represent the actual physical system under investigation, there should be no part lost or no new phenomenon introduced by the discretization. Minimization of numerical error as well as simulation time is always desired.

The disk's out-of-plane displacement under the slider is mathematically modeled here as an infinite series of sinusoids:

$$d(x) = \sum_{i=1}^{\infty} A_i \sin\left(\left(2p \big/ l_i\right)x - f_i\right) \qquad (1)$$

Where A_i are the amplitudes, λ_i are the wavelengths, and ϕ_i are the phase angles. A_i, and l_i , $(i=1,2,\ldots)$ in the bandwidth of 0-10 kHz are generally dependent on the spindle motor, clamping device, disk substrate material properties, disk geometry and rotational speed.

IV. ONCE AROUND DISTORTIONS: INITIAL SIMULATIONS

All simulations presented here were for the same pico-slider. This slider is a negative pressure five-pad design shown in Fig. 6. Additional simulations were also conducted for other ABS designs and showed similar results. The FH and FHM values shown in this paper are at the transducer location on the air bearing slider, which, for this slider, is located near the center trailing edge. Also, throughout this paper, spacing is referred to as the spacing between the transducer and the disk's surface underneath the transducer. FHM is the spacing with a zero mean.

The fundamental rotational out-of-plane displacement of the disk is represented by the simple sinusoid:

$$d_1(x) = A_1 \sin\left(\left(2p/l_1\right)x\right) \qquad (2)$$

As an example, A_1 is equal to 4 μm, disk rotational speed is 10,000 RPM, and λ_1 is related to the radial position, r = 45.6 mm by:

$$l_i = \frac{2pr}{k} \qquad (3)$$

where k is the number of wavelengths per revolution (for this case k equals 1). A simulation was conducted with the above disk input with a time step of 0.0005 ms. The FHM results are shown in Fig. 7. It is seen that FHM is present due to the once around disk motion with a peak-to-peak amplitude of 4.2 nm corresponding to 15 % of the FH. Therefore from these simulation results we find that significant variations in the FH can be caused by once around disk distortions. This result was somewhat unexpected, and it instigated further analysis.

V. DISK AND SLIDER MOTION: DERIVATION OF NUMERICAL FHM

From the theory of linear dynamical systems, significant FHM due to the disk's out-of-plane motion below 10 kHz should not be present. However, from the simulation results we find that significant FHM is present. Therefore we investigated the possibility of numerical errors in the simulation.

When the disk surface is discretized in the circumferential direction along the track it is transformed from a continuous track (equation (2)) to discrete space and time steps by:

$$d_1(\Delta xn) = A_1 \sin\left(\left(2p/l_1\right)\Delta xn\right) \qquad (n=0,1,2,\ldots) \qquad (4)$$

where Dx is the distance the disk travels under the slider within one time step iteration, Δt. Δx is related to Dt by:

$$\Delta x = \left(\frac{RPM * 2pr}{60}\right)\Delta t \qquad (5)$$

The relative linear velocity, v, can be related to the rotational speed, RPM, and the radial position, r, by:

$$v = \frac{RPM * 2pr}{60} \qquad (6)$$

In Figs. 8, 9, and 10 we show the disk surface under the slider generated by the discretization of a once around, 3 μm amplitude clamping distortion at three consecutive time steps for three values of Δt. These figures depict the discretized disk profile under the slider from the trailing edge to the leading edge of the slider, 1.25 mm in length on the positive slope of the sinusoid starting at t_o=0 sec. Three different time steps, 0.001 ms, 0.0005 ms, and 0.00005 ms are chosen to show how the disk surface is discretized for

different time steps. It is seen that for a larger time step (Fig. 8), resolution of the continuous sinusoidal disk waveform is lost and it becomes more of a sloped step function with a maximum step height of 4.2 nm.

The slope, $s_1(x)$ of $d_1(x)$ can be found by differentiation, and then it is discretized to find $s_1(x_i)$:

$$s_1(x) = \frac{\partial}{\partial x}\left(d_1(x)\right) = \frac{2A_1\pi}{l_1}\cos\left(\left(2\pi/l_1\right)x\right)$$

$$s_1(x_i) = \frac{2A_1\pi}{l_1}\cos\left(\left(2\pi/l_1\right)x_i\right) \quad (i=0,1,2,\ldots) \qquad (7)$$

where x_i is equal to Δxn (distance traversed over one iteration times the iteration number). The discretized slope can be used to find the step height at each adjacent time step seen in Figs. 8, 9 and 10. The step height, $y(x_i)$, is given by:

$$y(x_i) = s(x_i)\Delta x \qquad (i=0,1,2\ldots) \qquad (8)$$

The continuous sinusoidal disk clamping distortion being simulated is transformed into sloped step functions with a local slope found from equation (7) and adjacent step heights that can be found from equation (8) as seen in Fig. 8.

For simulations of a once around clamping distortion, this step height, $y(x)$, can be more than 5 nm. Under this circumstance the simulator is not modeling a continuous sinusoidal disk, but rather a series of step functions. To understand how this affects the spacing between the slider and the disk, and motivated by the initial simulations, we make the following assumption: it is assumed that the slider cannot respond instantaneously to the series of sloped step functions of the discretized disk's profile at a

frequency of 1/Δt, and therefore the FHM generated by the discretized sinusoid into step functions can be approximated by:

$$FHM_{numerical}(x_i) \approx -y(x_i) \qquad (i=0,1,2,\ldots) \qquad (9)$$

As will be seen, this assumption is valid for "step function like" disk surfaces. For long disk wavelengths, the disk profile under the slider is similar to that shown in Figs. (8) – (10). For shorter disk wavelengths, the disk profile no longer appears as sloped step functions under the slider and equation (9) is no longer valid. Therefore the wavelength of the disk surface has to be much larger than the slider length for this phenomenon to be present. This numerically generated FHM can now be estimated by using equations (7) and (8) in (9):

$$FHM_{numerical}(x_i) = -\left(\frac{2A_1 p v \Delta t}{l_1}\right)\cos\left(\left(2p/l_1\right)x_i\right) \qquad (10)$$

If this relationship is valid then the erroneous numerical FHM can be predicted and accounted for post-simulation. Using equation (10) for the above example of the once around clamping distortion, we can account for the 4.2 nm peak-to-peak FHM in Fig. 7. However, to accomplish the same approximation for complicated disk surface profiles, we will have to add together several functions, including their individual phase angles. The expanded form of equation (10) is:

$$FHM_{numerical}(x_i) = \sum_{j=1}^{n} -\left(\frac{2A_j p v \Delta t}{l_j}\right)\cos\left(\left(2p/l_j\right)x_i - f_j\right) \qquad (11)$$

We observe that the derived equation approximating this numerical FHM is proportional to A, v, and Δt, and it is inversely proportional to λ. If the derived equation is widely valid, it should predict correct results for all types of sinusoidal disk inputs provided the wavelength of the disk waviness is long compared to the length of the slider. Also, this numerical FHM is a specific function of A, v, λ, and Dt. The following simulations and calculations validate the derived equation for predicting this numerical FHM.

VI. SIMULATIONS

A. TWICE AROUND CLAMPING DISTORTION

We simulated the FHM for a twice around "potato-chip" clamping distortion. As an example, a 95 mm diameter disk clamped onto a spindle motor spinning at 7,200 RPM, A = 2.461 μm at a radial position of r = 45.6 mm and a time step of Dt = 0.0005 ms was simulated. The numerical FHM was predicted by equation (10). The simulation results and the predicted numerical FHM are plotted together in Fig. 11. The predicted numerical FHM matches very closely to the simulation results with only a 2.4 % difference. For this example, the simulation numerically generated FHM and the derived equation predicted FHM is 3.80 nm and 3.71, respectively, peak-to-peak, which is 30 % of the FH of 12.5 nm.

B. DEPENDENCE ON TIME STEP: 10X DISK FLUTTER

An example of how the time step alone affects this numerical FHM is provided by a ten-times around disk flutter. For this case, r = 45 mm, RPM = 10,020, and A = 0.4

μm. The time step, Δt, was decreased from 0.0006 ms to 0.00005 ms. The time steps of 0.0006 ms, 0.0004 ms, 0.0002 ms, 0.0001 ms, and 0.00005 ms were used in the simulation. Figure 12 presents the FHM simulation results shown for one wavelength of disk flutter. The peak-to-peak FHM values from both the simulations and the derived equation (10) are shown as a function of time step in Fig. 13. From these results, it is seen that the predicted FHM follows the simulation FHM and decreases linearly with decreasing time step. For the largest time step, Δt = 0.0006 ms, the peak-to-peak amplitude of this numerical FHM is 5 nm, 36 % of the FH. For the smallest time step, Δt = 0.00005 ms, the peak-to-peak amplitude of this numerical FHM is 0.42 nm, 3 % of the FH. Both the predicted and the simulation results have a zero intercept (actually 0.03 nm) showing that the FHM approaches zero with the time step as predicted. From this set of simulation results we can state the following:

$$FHM_{Physical} = \lim_{\Delta t \to 0} FHM_{numerical} = 0 \qquad (12)$$

As the time step approaches zero, the numerical FHM approaches zero correctly predicting the physical FHM. However, further simulations were carried out for the other dependent variables: v, A, and λ.

C. Dependence on Linear Velocity: Twice Around Clamping Distortions

The numerical FHM predicted by equation (10) shows a linear dependence on the relative linear velocity, v. In order to check this dependence, we simulated a twice around clamping distortion with an amplitude of 2 μm, radius of r = 45.6 mm and rotational speeds ranging from 5,000 RPM to 10,000 RPM with a time step of 0.0007 ms. Peak-to-peak values of the simulation and predicted FHM are shown in Fig. 14 as a function of linear velocity or RPM. Here the dependence of linear velocity on FHM is

shown to be linear as predicted. Also, as seen in Fig. 14, the intercept is approximately equal to zero showing the FHM approaches zero as the linear velocity approaches zero.

D. LIMITS OF THE DERIVED FORMULA: SWEPT SINE WAVE DISK TOPOGRAPHY

One fairly comprehensive test for the derived formula in equation (10) is the application to a sinusoidal disk function with changing amplitude and wavelength. Here we define the disk profile function:

$$d(x) = (\beta x + \gamma)\exp(-\chi x)\cos\left(\frac{2\pi}{\alpha x + \sigma} x\right) \qquad (13)$$

The variables $\beta, \gamma, \chi, \alpha, and \sigma$ were chosen to be: -4.42097e-6, 2.5e-6, 7, -0.5, and 0.28274, respectively. The disk profile function is shown in Fig. 15. These values were chosen to obtain a waveform with starting amplitude, A = 2.5 μm with a once around wavelength, λ = 0.2827 m. The ending distance was chosen to be 0.51 m corresponding to an amplitude of approximately 7 nm at a wavelength of λ = 3 mm, corresponding to approximately 15.7 kHz. The slope of $d(x)$ can be found by differentiating the above function or by using a finite difference approach. The numerical FHM can be found simply by using equations (8) and (9) and the digitized disk profile from the simulation:

$$FHM_{numerical} = -(d(x_{i+1}) - d(x_i)) \qquad (i=0,1,2,\ldots) \qquad (14)$$

This waveform exercises the dependence of this numerical FHM on the amplitude and wavelength of the disk profile. Also, simulations were performed for time steps of Δt = 0.0007 ms, 0.0005 ms, 0.0003 ms and 0.0001 ms to test the dependence on the time step.

From these four simulations, the derived formula can be tested for its dependence of all except one variable (Δt, A, and l).

The predicted and simulation results from these simulations are plotted together in Figs. 16, 17, 18 and 19. Notice that these figures are plotted on the same scales and as the time step decreases, so do the FHM amplitudes. From these results, it is shown that the derived numerical FHM equation (10) holds for wavelengths from once around clamping distortions down to λ = 6 mm corresponding to 1/47 of the distance around the disk circumferentially, or a frequency of 7.9 kHz. When the disk waviness wavelength is reduced below 6 mm the assumption of it being much longer than the slider's body no longer holds, as seen from Figs. 16-19. Notice from the results for the time step of 0.0001 ms shown in Fig. 19, the simulation FHM is slightly different from the predicted FHM for wavelengths less than approximately 16 mm (beyond the distance of approximately 0.3 m). This phase shift between the predicted and simulation results stems from geometric FHM [1]. The simulated disk profile, slider motion and the spacing are shown for a time step of 0.0001 ms in Fig. 20. It shows that for disk waviness wavelengths less than 6 mm (distance greater than 0.49 m), the spacing modulation increases monotonically. This phenomenon is not predicted by equation (10) and is therefore not related to discretization in the simulation. It is physically expected however; it is due to geometric FHM [1]. Geometric FHM is not dynamic excitation of resonance of the air bearing film but a phase shift and decreasing amplitude in the slider's response to the disk's input. Also, from these results it is observed that for time steps greater than 0.0001 ms, the geometric FHM is not accurately predicted in the simulation.

VII. EXPERIMENTAL MEASUREMENT

In previous investigations, we developed and utilized a system to measure FHM in the frequency bandwidth from 10 kHz to 2 MHz with extremely high resolution [3,4]. Disk morphology and other repeatable events that cause out-of-plane motion of the disk have amplitudes of several nanometers in the frequency bandwidth greater than 10 kHz. The demonstrated 90-95 % repeatability translates into sub-nanometer resolution of the measurement system [3,4]. The FHM that could be associated with the disk clamping/warping/flutter are low frequency, high amplitude displacements that present a different measurement problem. As an example, for a once or twice around clamping distortion with amplitude of 2.5 μm, a repeatability of 95 % can introduce an error of ± 125 nm. In order to decrease the error to sub-nanometer levels it is necessary to use a dual beam or differential beam LDV measurement. A schematic diagram of this procedure is shown in Fig. 21. This measurement yields the relative motion (velocity or displacement) between the two laser spots. This procedure is discussed in detail by Zeng *et al.* [3]. Several measurements were taken of the disk's motion on the outer diameter of the disk as depicted in Fig. 21. The beams were positioned as close together as the optics would allow (approximately 250 μm). Three sets of data are shown in Fig. 22. It is expected that all these measurements would be exactly the same, and 95 % repeatability is obtained, which is still a large enough difference to produce a ± 5 nm error. Unfortunately, this measurement system also cannot obtain the needed resolution to verify the simulation and derived findings of this paper. The bandwidth of sub-nanometer resolution for this measurement system is from 7-8 kHz to 2 MHz, which is above the bandwidth of interest here.

VIII. DISCUSSION AND CONCLUSION

In previous studies, FHM in the bandwidth of 10 kHz to 2 MHz has been discussed and verified both experimentally and by simulation. From the theory of linear dynamical systems, it is expected that FHM below 10 kHz should not be present with significant amplitude. However the initial numerical simulations showed that FHM was present due to much lower frequency once around clamping distortions. Rotating disk dynamics as seen by a stationary observer in the frequency range of DC to 10 kHz were discussed. It was shown that the clamping distortions, spindle vibrations and disk flutter all produce relatively low frequencies and high amplitudes – on the micron level. It was also shown that when simulating disk clamping distortions and flutter the disk surface is discretized from a continuous sinusoid into a series of sloped step functions that depend on the time step and cause errors in the simulation. An equation was derived to approximate this erroneous numerical FHM by assuming it results from the disk step heights between adjacent time steps. This equation predicted the numerical errors for disk waviness wavelengths that are much longer than the slider's body length. The error was found to be proportional to the linear disk velocity, time step, and amplitude of the disk waviness, and it is inversely proportional to the waviness wavelength.

Various simulations verified the derived equation for predicting this numerical FHM using the CML Dynamic Air Bearing Simulator. Initially, a twice around clamping distortion was simulated and the results were compared to the derived predicted results showing excellent correlation. The dependence on time step was then verified by using a ten-times around disk flutter for various time steps. The simulation results for two and

ten wavelengths per circumference agreed with the predicted results, showing that the FHM error vanishes as the time step approaches zero:

$$\lim_{\Delta t \to 0} FHM_{numerical} = 0 \qquad (15)$$

The dependence on disk velocity was verified by simulating a two wavelength clamping distortion with several different rotational speeds. These simulations showed the predicted linear dependence on velocity of the numerical FHM. A variable wavelength disk topography function was introduced to exercise the dependence on all except one variable. The disk function represented continuously decreasing amplitudes and wavelengths from one to 50 wavelengths per circumference. From these simulations, it was shown that the equation predicted the erroneous numerical FHM for wavelengths down to 6 mm. Below 6 mm, the derived equation was no longer valid – there the waviness wavelength is no longer much larger than the length of the slider. Also, for wavelengths smaller than approximately 6 mm, the well understood geometric FHM becomes pronounced.

From the results presented in this paper, we concluded that an erroneous numerical FHM exists and can be accounted for when modeling disturbances at frequencies below 10 kHz. In order to accurately numerically simulate the effects of the low frequency disk's waviness, a time step of 0.0001 ms or less is required.

ACKNOWLEDGEMENT

This work was supported by The Computer Mechanics Laboratory at the University of California, Berkeley, USA and the National Storage Industry Consortium (NSIC).

REFERENCES

[1] B.H. Thornton, A. Nayak, and D.B. Bogy, "Flying Height Modulation Due to Disk Waviness of Sub-5nm Flying Height Air Bearing Sliders," J. of Tribology, accepted for publication.

[2] B.H. Thornton, and D.B. Bogy, "Dynamics of a High RPM Hard Disk Drive in Operation," Technical Report No. 00-001, Computer Mechanics Lab, Dept. of Mechanical Engineering, UC Berkeley, January 2000.

[3] Q.H. Zeng, B.H. Thornton, D.B. Bogy, and C.S Bhatia, "Flyability and Flying Height Modulation Measurement of Sliders with Sub-10nm Flying Heights," IEEE Trans. on Mag., Vol. 37, No.2, pp. 894-899, March 2001.

[4] B.H. Thornton, and D.B. Bogy, "The Effects of Disk Morphology on Flying-Height Modulation: Experiment and Simulation," TMRC 2001, invited paper. IEEE Trans. on Mag., accepted for publication.

[5] L.-Y. Zhu, and D.B. Bogy, "Head-Disk Spacing Fluctuation due to Disk Topography in Magnetic Recording Hard Disk Files," Tribology and Mechanics of Magnetic Storage Systems, STLE Special Publication, SP-26, 1989, 160-167.

[6] C. Denis Mee, and E. D. Daniel, "Magnetic Recording Handbook," McGraw Hill, 1987.

[7] J. S. McAllister, "The Effect of Platter Resonances on Track Misregistration in Disk Drives," S/V Sound and Vibration, pp. 24-28, January 1996.

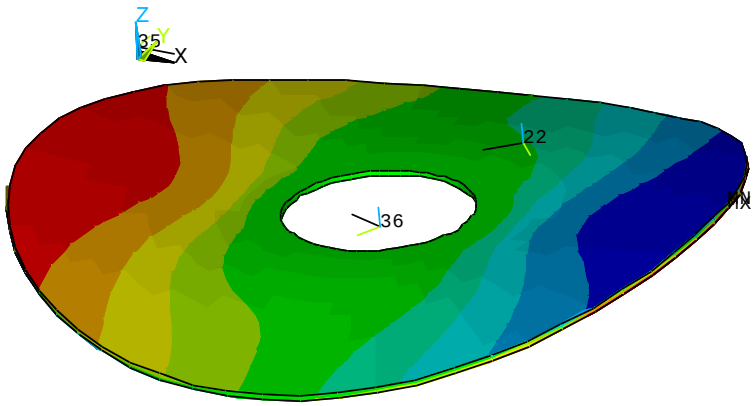

Fig. 1: Deformed shape of the "potato chip" clamping distortion.

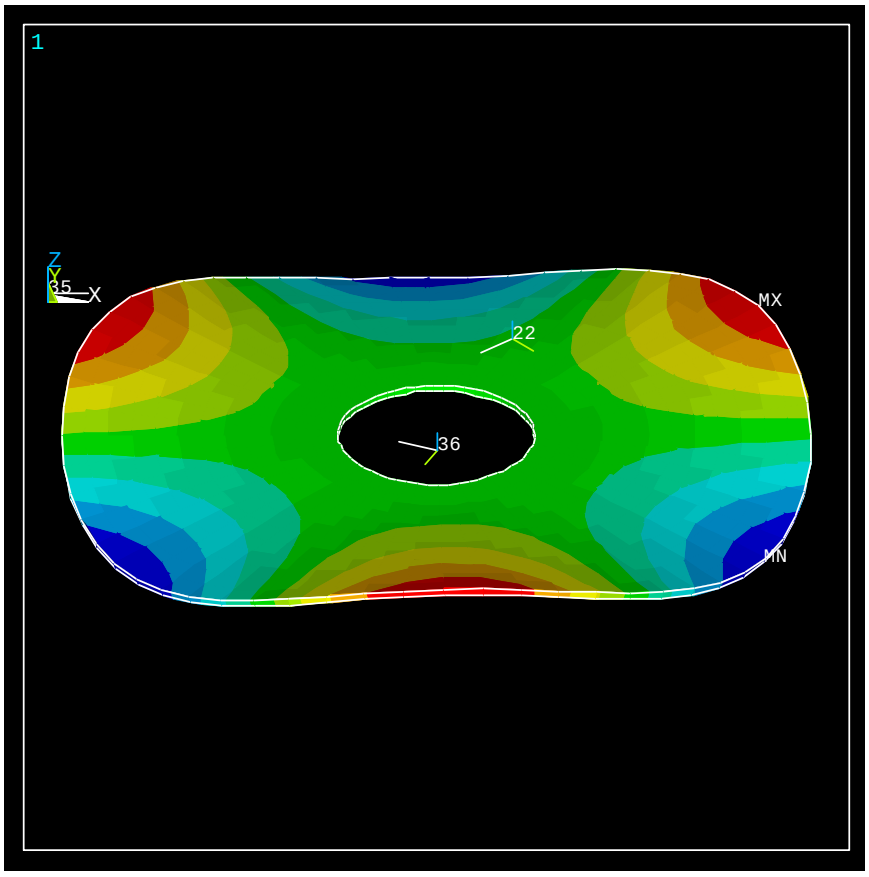

Fig. 2: Deformed shape of the (0,3) disk mode at 1170 Hz.

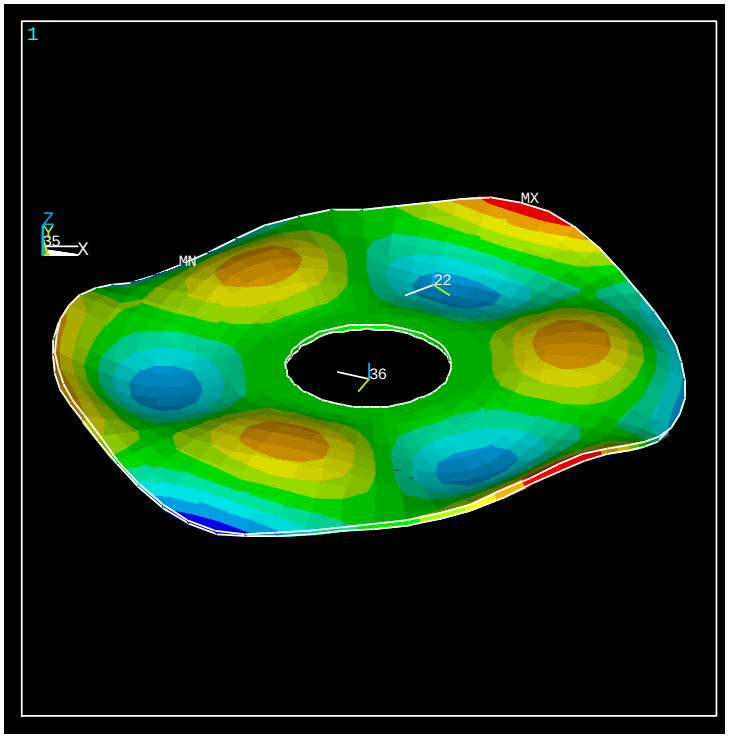

Fig. 3: Deformed shape of the (1,3) disk mode at 5724Hz.

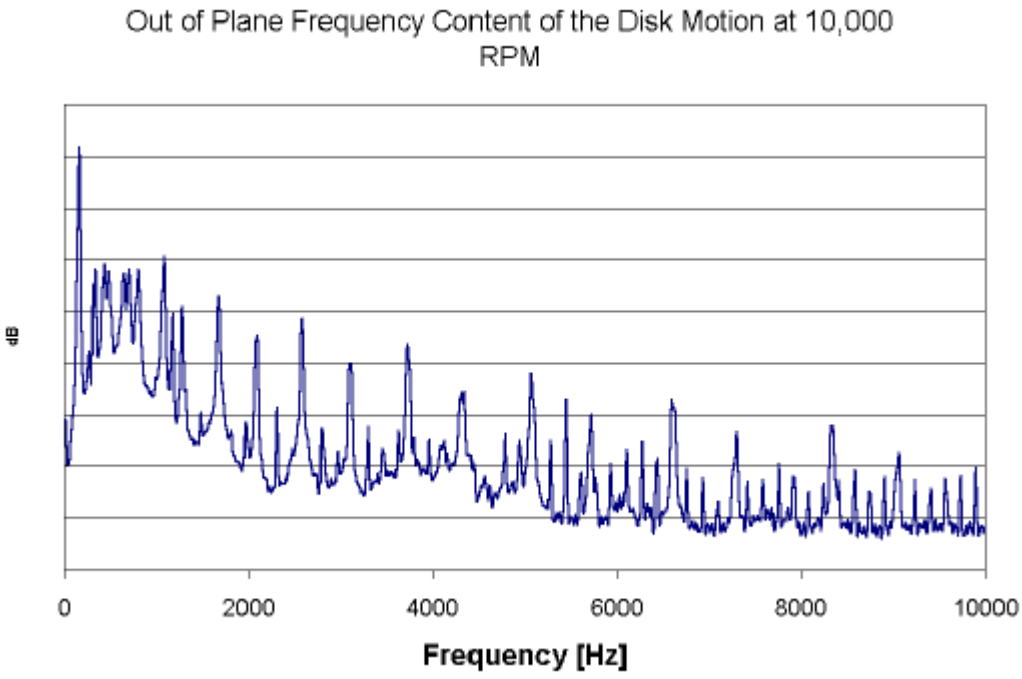

Fig. 4: Out of plane frequency content of the disk motion spinning at 10,000 RPM measured by LDV.

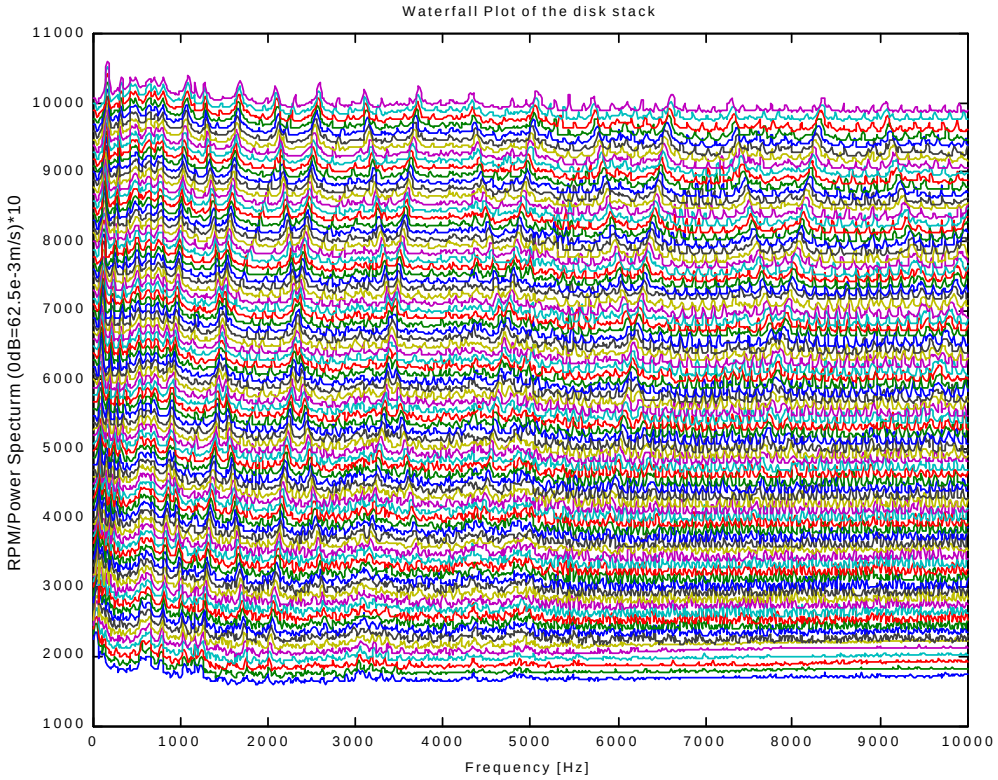

Fig. 5: Spin-up waterfall plot of the out of plane disk motion measured with LDV.

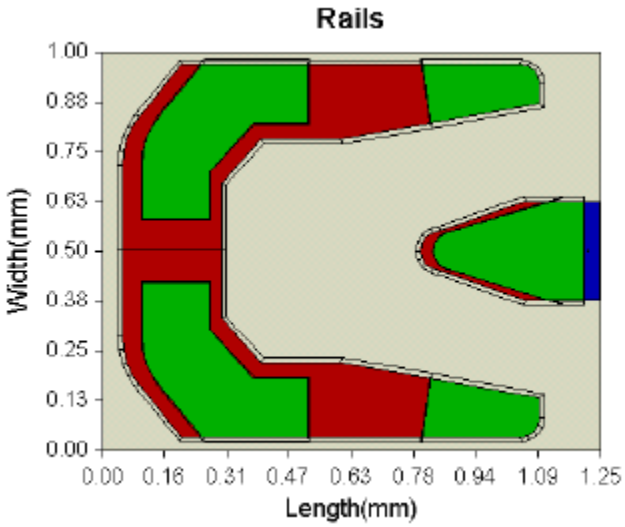

Fig. 6: Pico air bearing slider surface used in simulations.

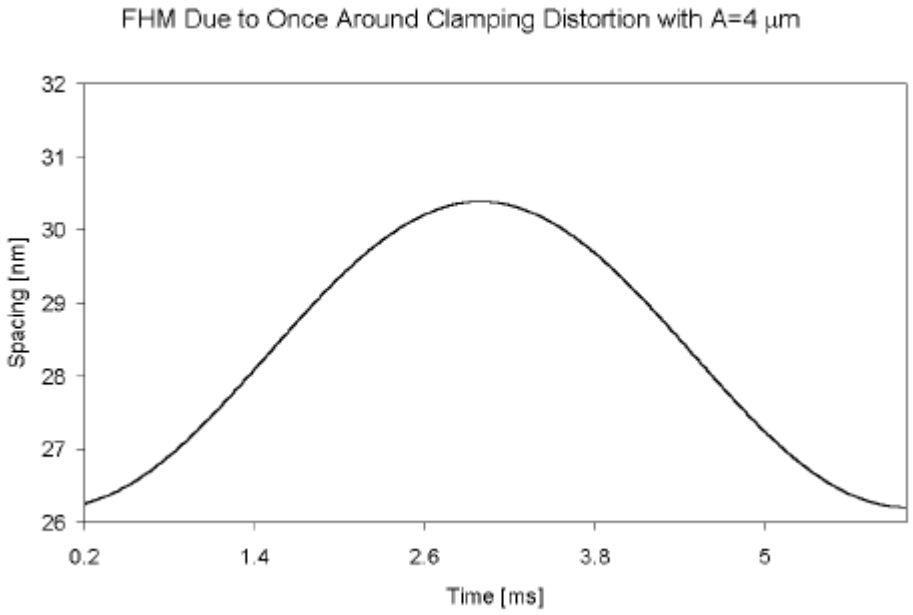

Fig. 7: FHM due to once around clamping distortion with amplitude of 4 mm. Spacing shown for one revolution.

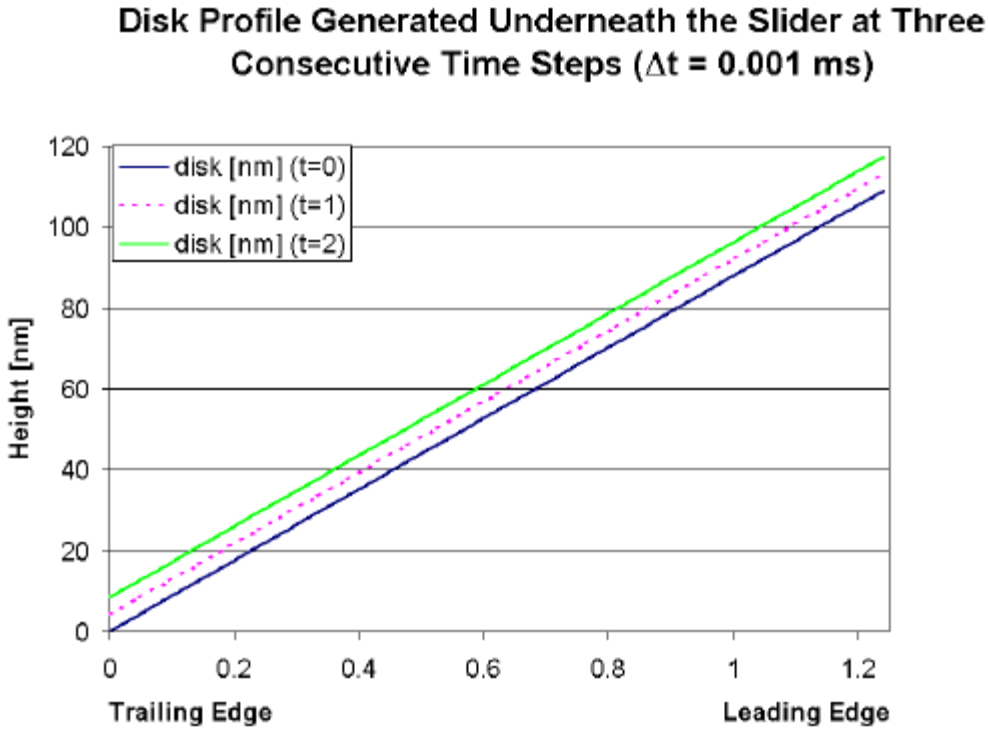

Fig. 8: Disk profile generated underneath the slider at three consecutive time steps for a Dt = 0.001 ms.

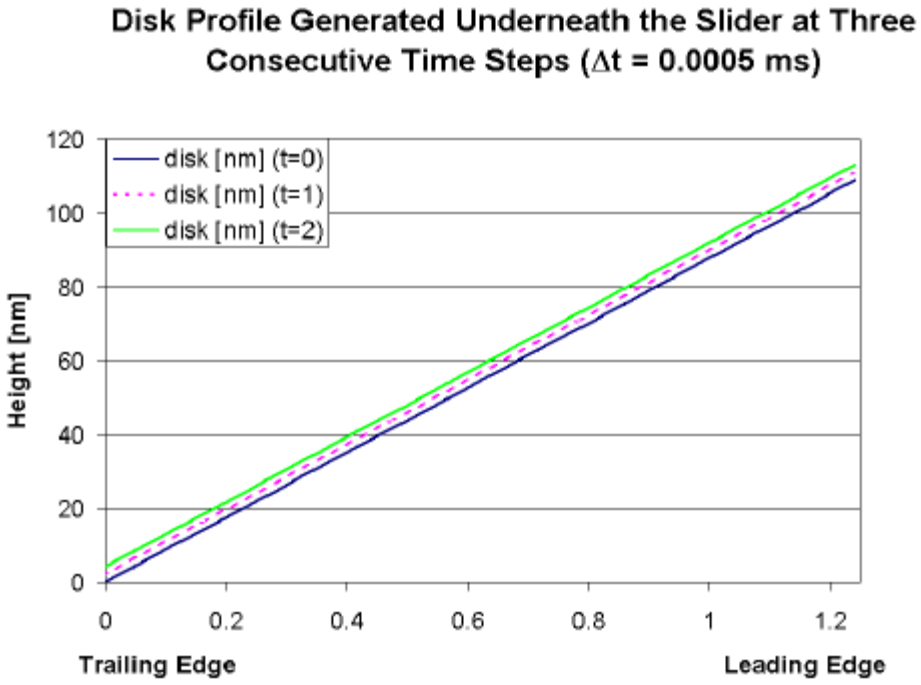

Fig. 9: Disk profile generated underneath the slider at three consecutive time steps for a Dt = 0.0005 ms.

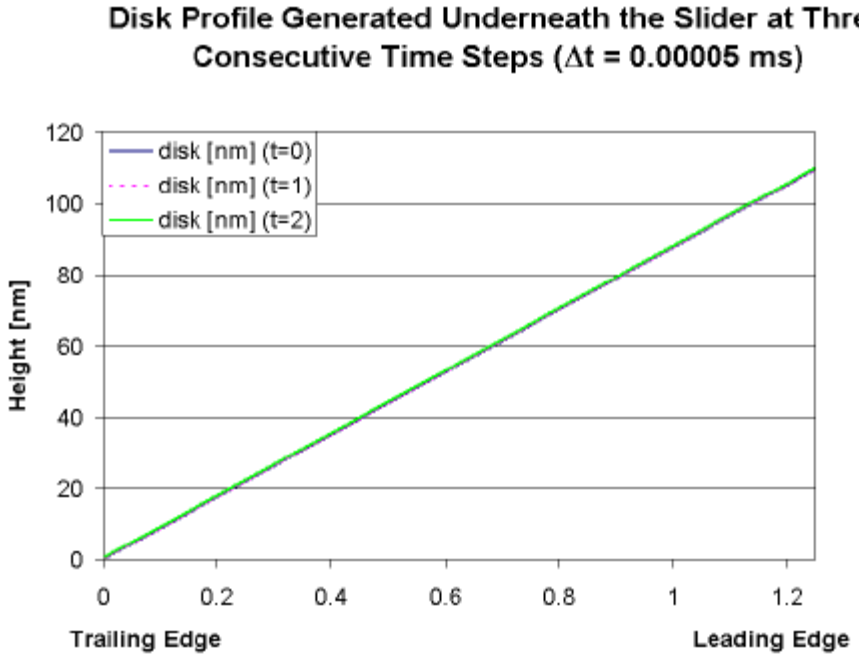

Fig. 10: Disk profile generated underneath the slider at three consecutive time steps for a Dt = 0.00005 ms.

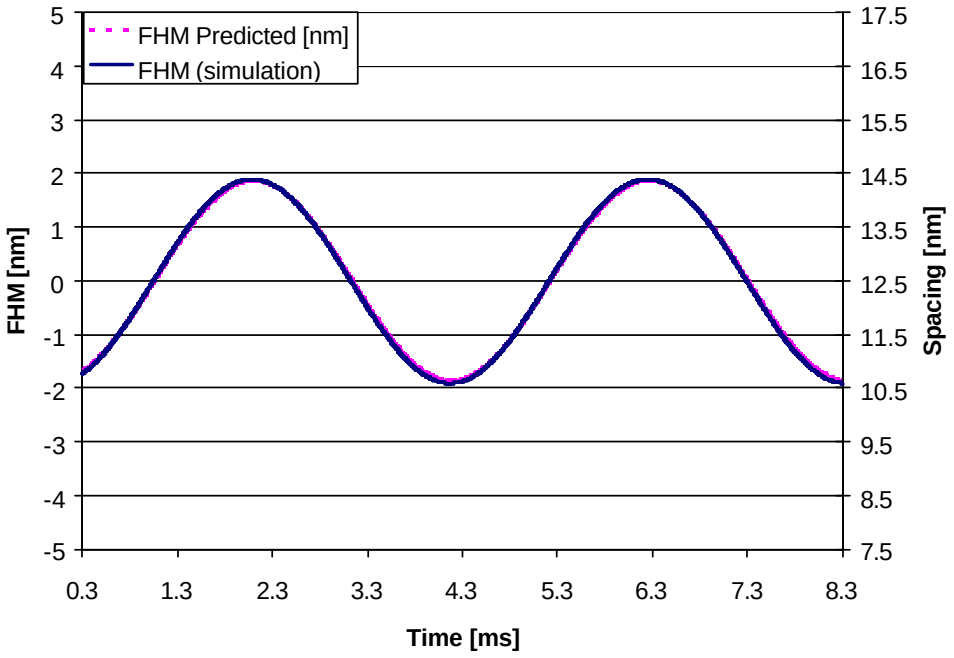

Fig. 11: FHM simulation and predicted results for a twice around clamping distortion.

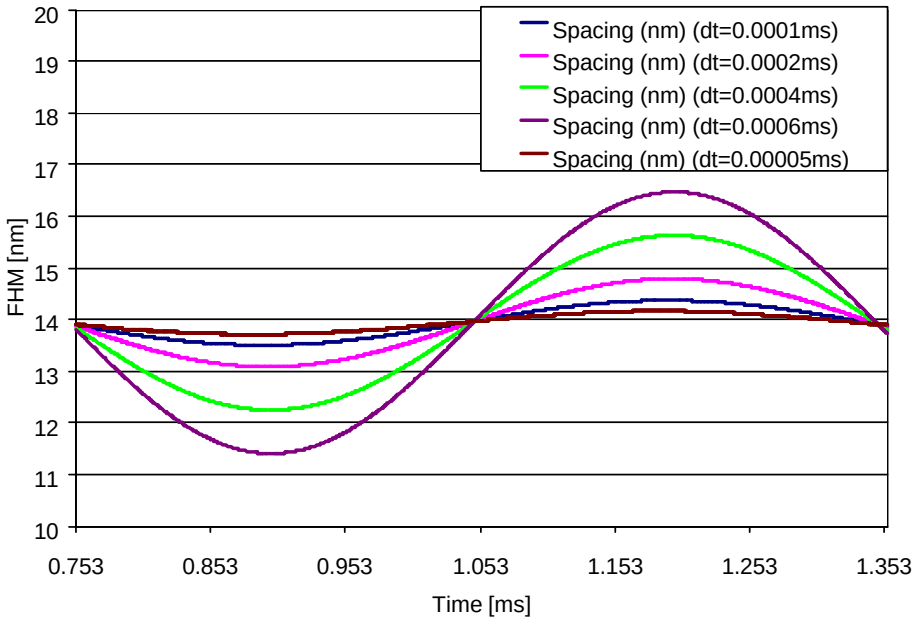

Fig. 12: Spacing simulation results for a 10X clamping distortions shown for one wavelength of waviness and for different time steps.

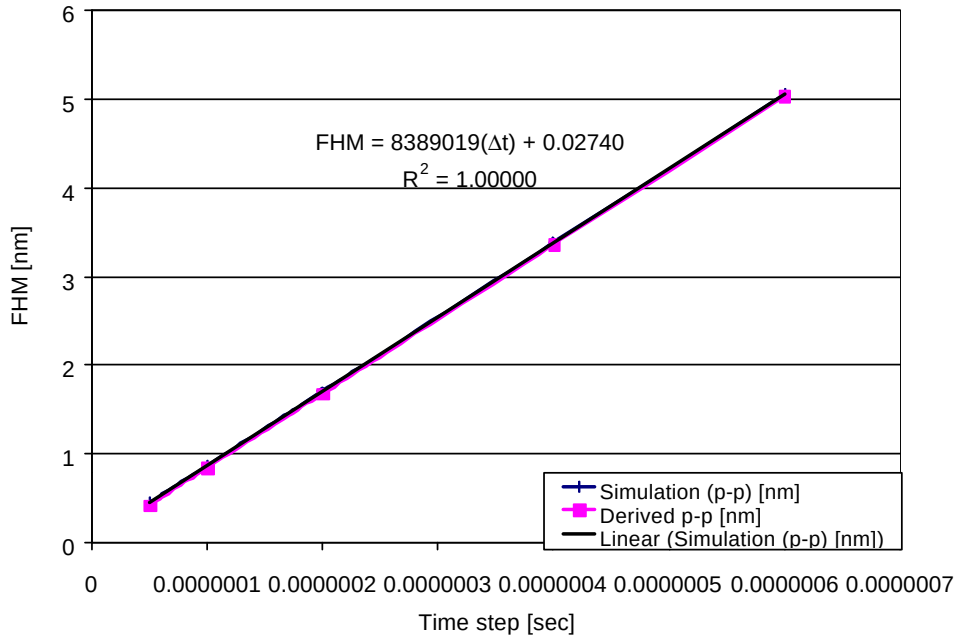

Fig. 13: Summary of the FHM from simulation and prediction for a 10X clamping distortion as a function of time step.

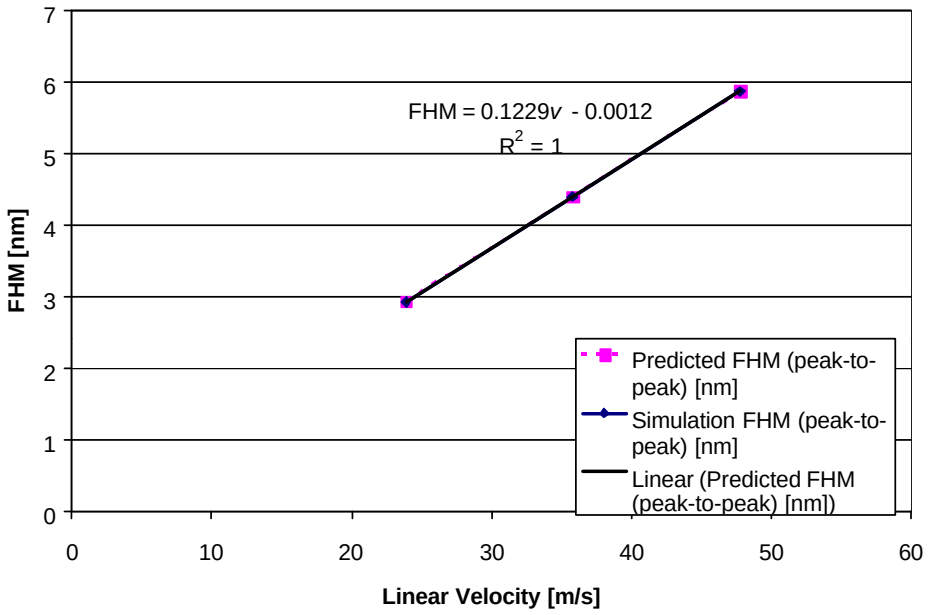

Fig. 14: FHM as a function of linear velocity for a twice around clamping distortion shown for both the simulation and predicted results.

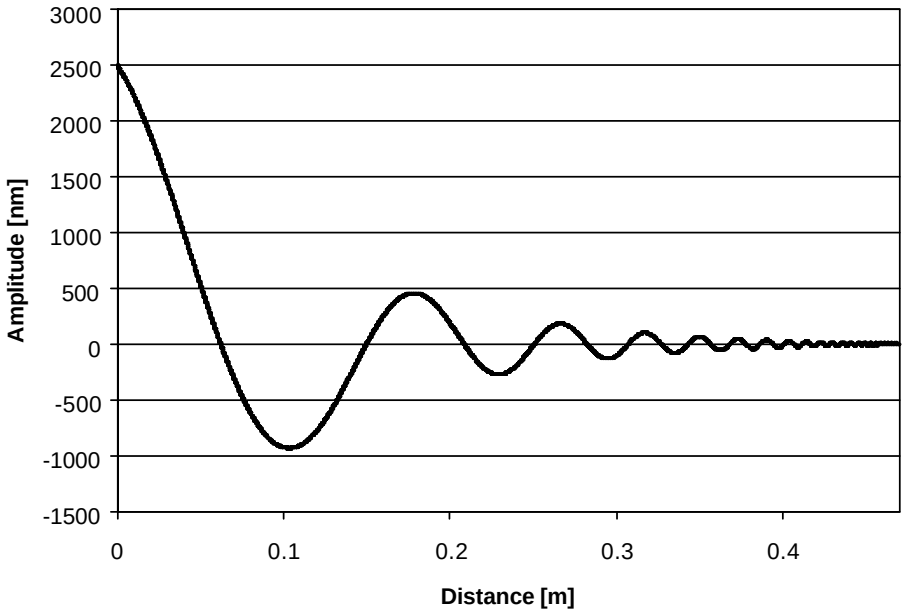

Fig. 15: Disk function.

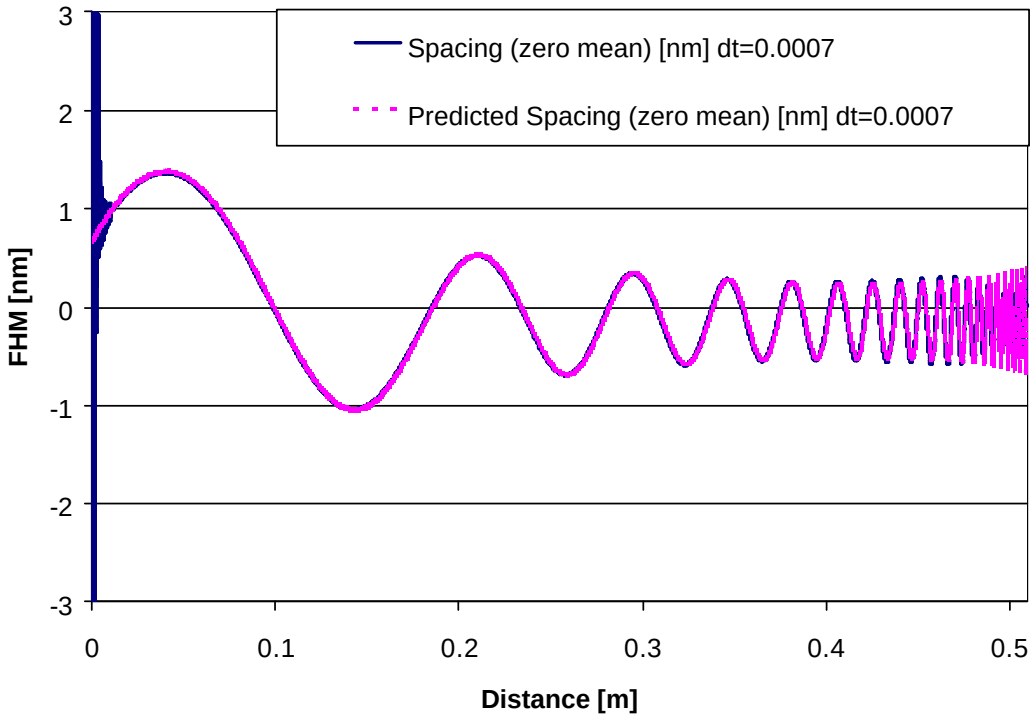

Fig. 16: Simulation and predicted FHM due to the disk function shown in Fig. 15 for a time step of 0.0007 ms.

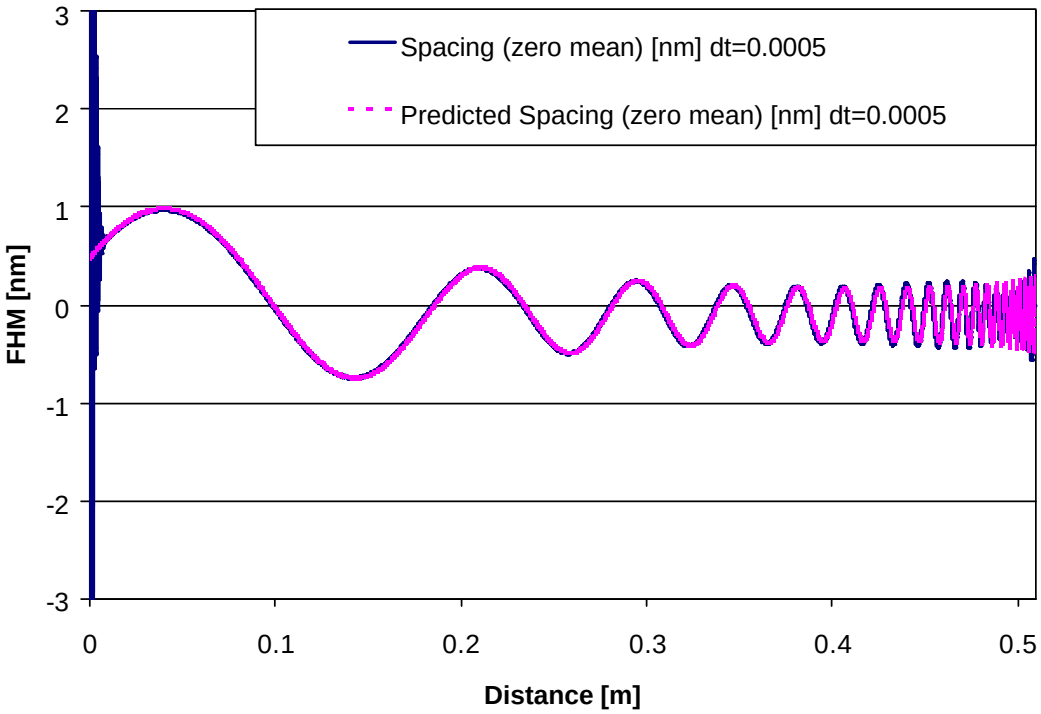

Fig. 17: Simulation and predicted FHM due to the disk function shown in Fig. 15 for a time step of 0.0005 ms.

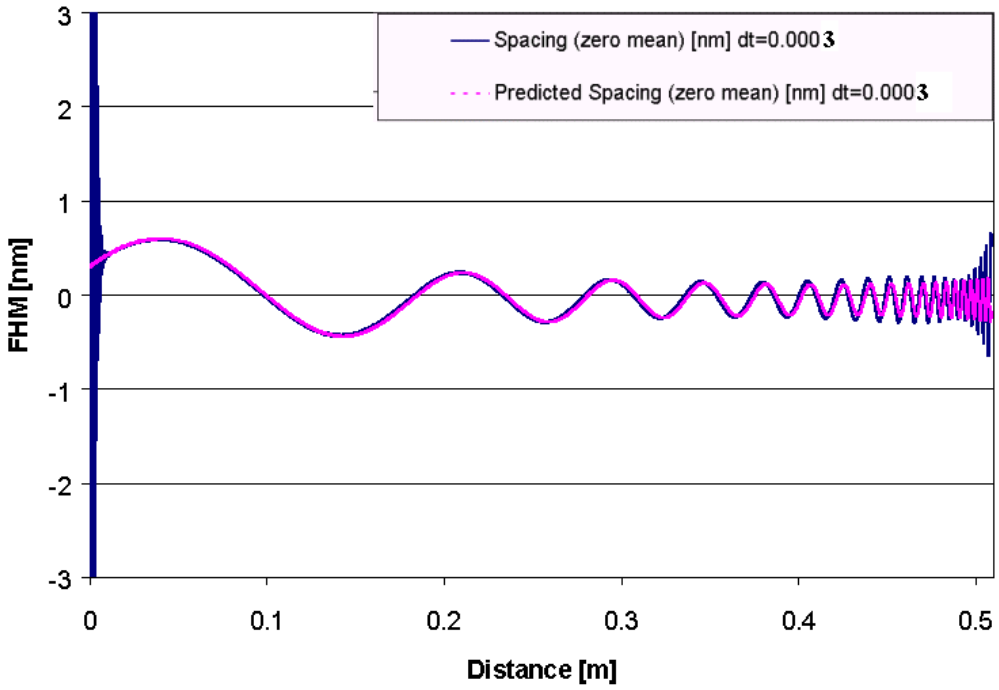

Fig. 18: Simulation and predicted FHM due to the disk function shown in Fig. 15 for a time step of 0.0003 ms.

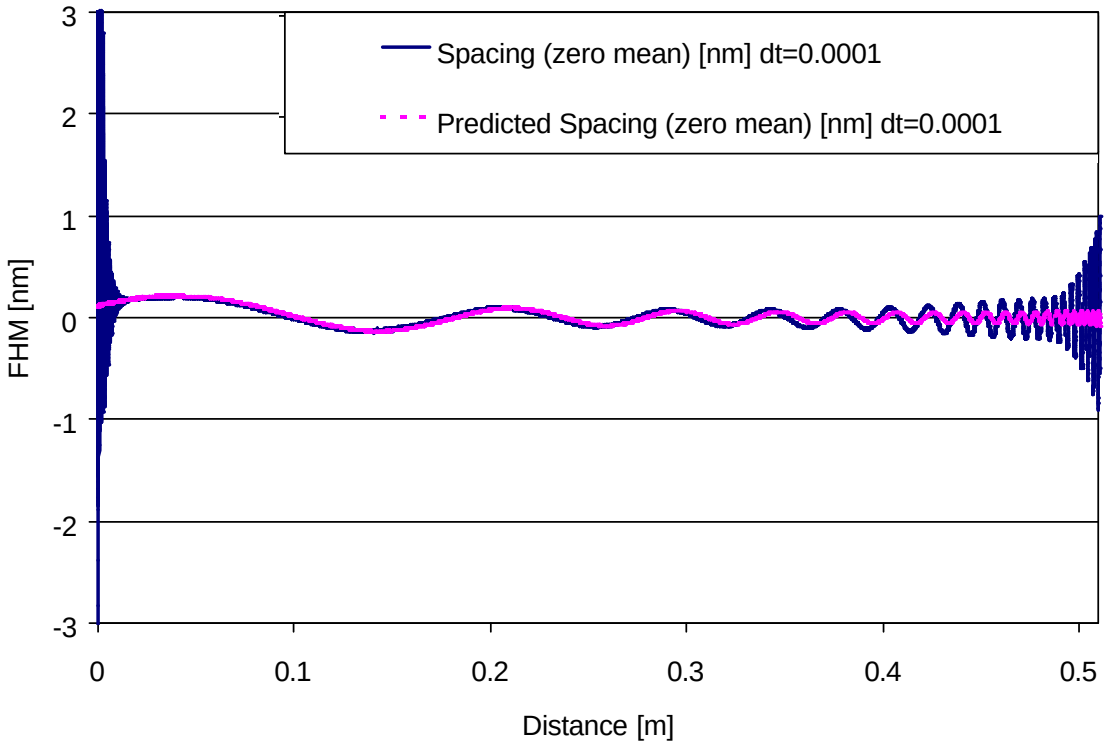

Fig. 19: Simulation and predicted FHM due to the disk function shown in Fig. 15 for a time step of 0.0001 ms.

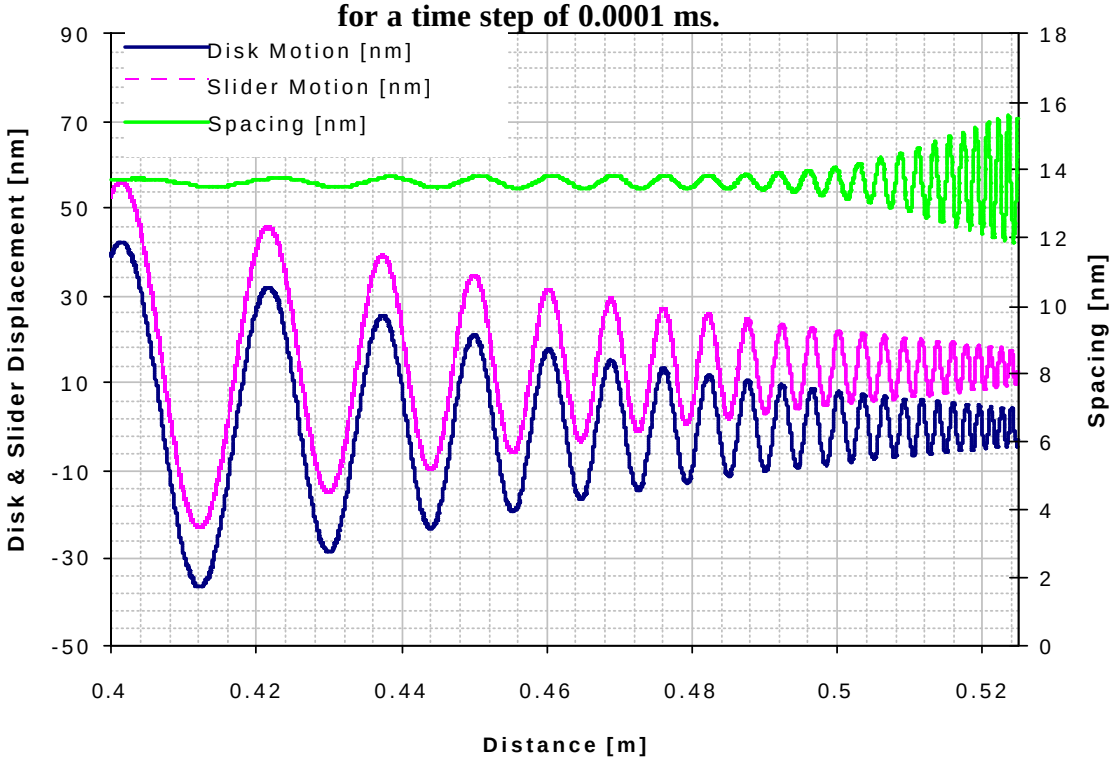

Fig. 20: Simulation results of the disk and slider displacements and the spacing for a time step of 0.0001 ms.

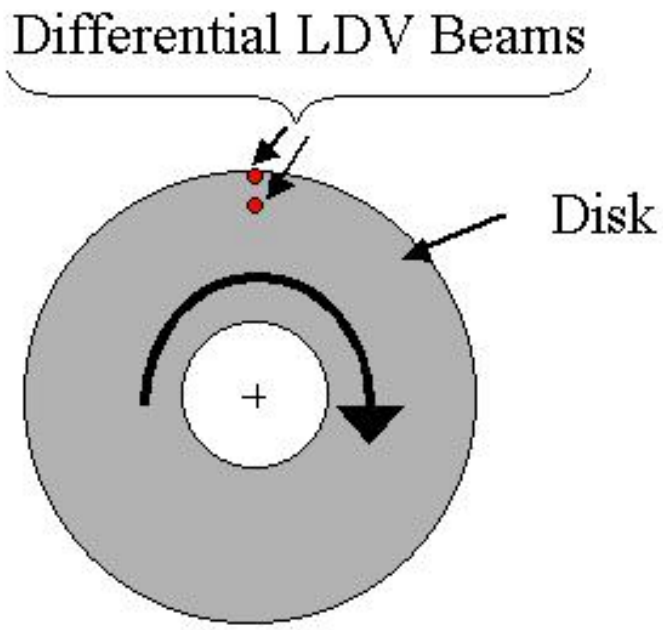

Fig. 21: Experimental Schematic of the differential LDV beam measurement of the disk out of plane motion.

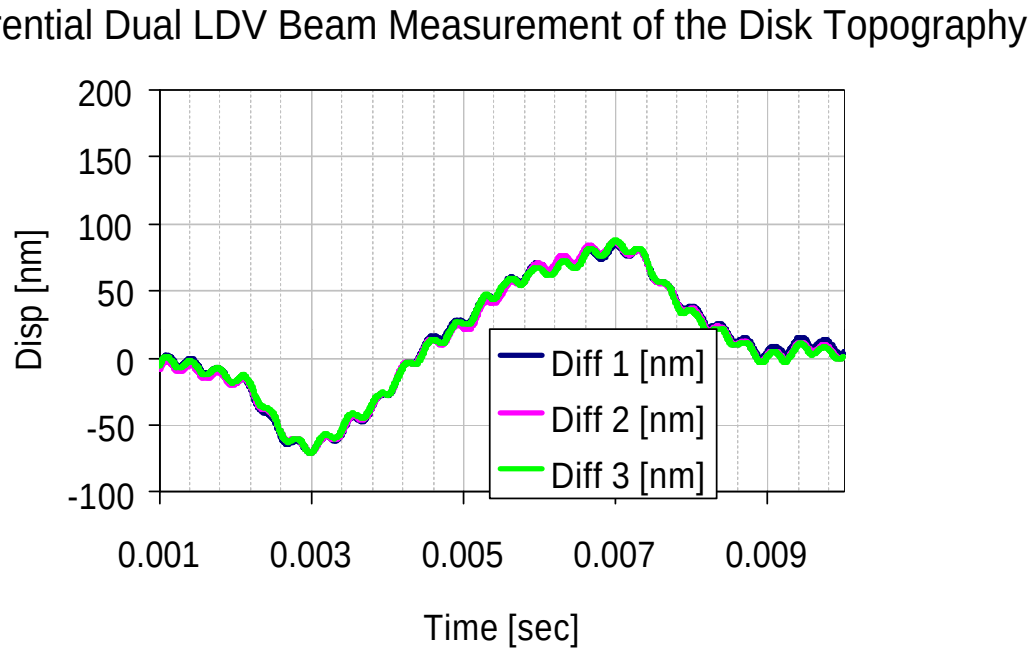

Fig. 22: Three experimental measurements of the disks topography.